POAC'23
Glasgow, United Kingdom

Proceedings of the 27th International Conference on
Port and Ocean Engineering under Arctic Conditions
12-16 June 2023, Glasgow, United Kingdom

A growth model for aqueous model ice

Silvano Rosenau[1], Nils Reimer[2], Dirk Notz[1], Franz von Bock und Polach[3]
[1]Institut für Meereskunde, Universität Hamburg, Hamburg, Germany
[2]The Hamburg Ship Model Basin (HSVA), Hamburg, Germany
[3]Institute of Ship Structural Design and Analysis, Hamburg University of Technology, Hamburg, Germany

ABSTRACT

Experimental testing in model ice is still the state-of-the-art method for the performance prediction of ships and structures in ice. For frequently produced ice thicknesses large experience is available to estimate the growth rate and the final thickness. However, the prediction of growth rate for model ice thicknesses outside this range come with major uncertainties. An accurate growth prediction of the ice requires a physical growth model that can account for the complex boundary conditions. Such a model is also useful when boundary conditions change, for example the renewing of the cooling system. In this work, we propose a growth prediction model for model ice in The Hamburg Ship Model Basin (HSVA). In the HSVA, the ice is artificially seeded during the beginning of ice growth to modify the mechanical properties of the ice. We used a traditional thermodynamic ice growth model and modified it so that it takes the seeding procedure into account. We used measurements of air temperature and ice thickness to tune the tank specific model parameter. For the best fitting parameters, the mean squared difference between our model and measurements is 2.17 mm. We speculate that most of this difference is due to a strong post-growth that is not correctly represented in the model. Nevertheless, the model provides a significant improvement and help for the modelling of thin ice. By modelling the post-growth process individually, the model could be further improved. This, however, requires more measurements of the ice thickness during post-growth.

KEY WORDS Aqueous Ice; Ice Model; Ice Growth.

INTRODUCTION

The physical environment of sea ice is modeled in special facilities to test the behavior of ships and structures in sea ice. Since these test objects are scaled, it is essential to scale the mechanical properties of the ice as well. Over the past decades, various techniques have been developed in order to achieve the correct strength and breaking behavior of the ice. We refer to this artificial ice as aqueous ice. To weaken the ice structure, dopants (chemical additives) are added to the tank water, the seed water spray or both. These additives are dissolved in small concentrations either directly in the tank water, or separately in water and then sprayed as fine vapor above water surface. The water molecules crystallize in the air and settle as nuclei on the tank surface, where the dopants are entrapped in the ice. The different methods of model ice production differ by the dopants used (e.g., sodium chloride, ethanol) (von Bock und Polach,

et al., 2019) and in the duration of spraying. Spraying is the term used, when granular ice is produced by several crystal layers (Enkvist & Makinen, 1984), whereas seeding is the term used, when ice nuclei are seeded initially from which model ice with a fine columnar structure grows into the water (Evers, 1993). This process is in scale similar to sea ice growth that consists of a granular layer at the top and a columnar layer below (von Bock und Polach, et al., 2019).

The analytical and theoretical description of the growth process of aqueous ice is limited and the making of model ice is largely based on experience. Consequently, ice sheet productions for desired ice properties that are outside the realm of experience are subject to partly significant variations (von Bock und Polach, et al., 2019). This problem became evident in a test series for wave ice-interaction (Klein, et al., 2021), where the so called MIVET (Model Ice of Virtual Equivalent Thickness) was produced, which has a target thickness below 10 mm (von Bock und Polach, et al., 2021). Treating this issue, the aim of this study is to develop a prediction model for the growth of aqueous ice.

Although there exists a variety of different numerical models for ice growth in natural water bodies (Launiainen & Cheng, 1998), none of these models take the special conditions of ice growth in ice tanks into account. Here, we develop a model that is designed to predict the ice growth in The Hamburg Ship Model Basin (HSVA). The ice in the HSVA consists of a granular top layer and a columnar bottom layer and is generated by seeding a high density of ice nuclei onto the water surface from which the ice growth into the tank water which has a salinity of 7ppt. Consequently, the structure mimics sea ice in scale. Most recently, Nkoko Nossa, et al. (2015) developed an ice model that was tested in the ice tank of the HSVA. However, this study was not about the growth of aqueous ice but about the growth of first year ice in the ocean. Therefore, the ice-weakening processes in the HSVA were not considered. Consequently, no growth prediction model exists that allows a reasonable accurate prediction of aqueous ice growth. Especially for the growth of thin ice, where small deviations from target values have a higher impact. Furthermore, the corrective controlling of the growth is more difficult due to the growth dynamics.

In the first part of this paper, the methods section, we describe the ice growth prediction model. We first derive a thermodynamic model that gives the ice growth as a function of the cooling duration for a given air temperature. Afterwards we invert the model, such that it gives the cooling duration that is necessary to grow ice of a specified thickness at a given cooling temperature. To optimize predictions of ice growth in the HSVA, we tune the model with measurement data. In the first part of the results section, we present the results of the parameter tuning. Finally, we apply the prediction model by predicting the cooling duration that is necessary to grow a 7 mm thick ice sheet. The obtained ice was 2.7 mm thicker than the expected target value. In the second part of the results section, we argue that a major part of this error is due to an incorrect thermal conductivity between ice and air during temperature adjustment.

METHODS

The goal of this work is to develop a prediction model for the cooling duration that is necessary in order to grow ice of a certain thickness. For that, we use a thermodynamic ice growth model based on Anderson (1961) that calculates ice growth from air and water temperature. We include the granular ice layer as a constant ice layer that sits on top of the columnar ice and assume that the granular ice layer always takes the same amount of time to grow. In the section ‘Thermodynamic ice growth model’, we describe the ice growth model. Afterwards in

‘Prediction of cooling duration section’, we invert the ice growth model to get a prediction model of the cooling duration. Finally, in ‘Parameter estimation’, we tune model parameters with existing measurements of the ice thickness and air and water temperature.

Experimental facility

The ice tank is the Large Ice Model Basin (LIMB) of The Hamburg Ship Model Basin (HSVA) and is a rectangular basin of 70m by 10m with a water depth of 2.5m and a 12m long deep section with water depth of 5m. The temperature in the LIMB can be adjusted within a range of -20°C to plus 5°C. The model ice is generated by spraying a fine water mist onto the water surface where it settles as ice crystal and acts as seed. Then the ice grows downward into the saline water (7ppt of salt).

Thermodynamic ice growth model

Aqueous model ice comprises of two ice layers, granular ice at the top with a random grain orientation and columnar ice at the bottom with a predominant grain orientation (horizontal c-axis) (Fig. 1). The growth process of the two layers is fundamentally different: While the columnar ice grows downward at the bottom of the ice due to freezing water, the granular ice grows upward at the top due to freezing water vapor. This difference makes the modeling of aqueous ice growth challenging; Different models are necessary for each ice layer.

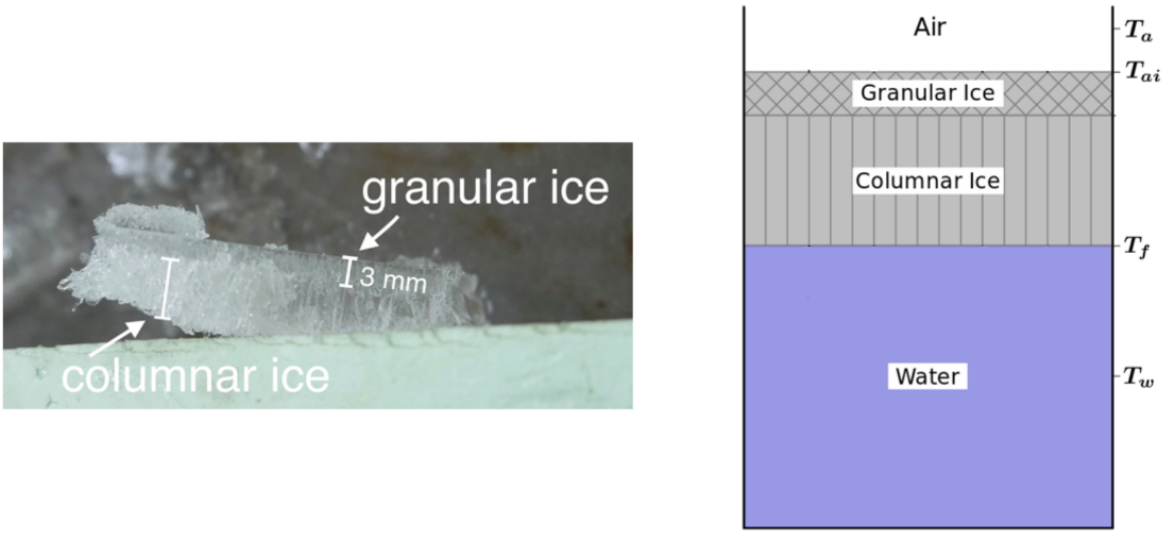

Figure 1. Right: Sidecut of aqueous ice. Left: Schematic of aqueous ice with T_a: air temperature, T_{ai}: air-ice-interface temperature, T_f: freezing point, T_w: water temperature.

At the present time, no approaches have been made to model the growth of the granular ice layer. In this work, we model the granular ice with the simplest statistical model that exists: We assume that the growth of the granular ice is always the same, meaning that it always takes the same amount of time to grow and always reaches the same thickness. By doing so, we take the granular ice layer into account in the aqueous ice model as a constant ice layer on top of the columnar ice. This zero order approach has much potential for improvement, however, for that, more measurements of the granular ice layer are necessary. Since the columnar ice layer is much thicker than the granular ice, we focus on the growth of the columnar ice layer in the aqueous ice model.

The growth process of columnar ice is similar to the growth process of sea ice. For this reason, we use a modified sea ice model (Anderson, 1961) to model the growth of columnar ice. The columnar ice grows, when the necessary enthalpy of fusion is dissipated from the water-ice interface. The ice model is based on this concept. It calculates the net enthalpy flux at the water-ice interface and from this the corresponding ice growth:

$$\rho_i L \frac{dh}{dt} = \Delta Q \tag{1}$$

(h: ice thickness, ρ_i: density ice, L: latent heat of fusion, ΔQ: net enthalpy flux).

To calculate the net enthalpy flux, we first assume that the ice has no thermal inertia and no heat sources/sinks. From this follows, that all the heat that enters the ice at the bottom must simultaneously leave the ice at the top. Hence, the net enthalpy flux is the difference of all enthalpy fluxes between water and ice as well as all enthalpy fluxes between ice and air. Enthalpy fluxes between ice and air are the radiative terms (incoming shortwave radiation, incoming and outgoing longwave radiation), the latent and sensible heat flux as well as the turbulent heat flux. We assume that the incoming and outgoing longwave radiation balance each other since the ceiling and the ice surface have similar temperatures. Further, we neglect the incoming shortwave radiation as the tank is roofed. We neglect the latent heat flux which is small because the air cannot capture much moisture at low temperatures. We neglect the sensible heat flux as it is multiple orders smaller than the turbulent heat flux. See Rosenau (2022) for a more detailed discussion on the heat fluxes. The turbulent heat flux equation is given by:

$$Q_a = -\kappa_t \frac{dT}{dz} \tag{2}$$

(κ_t: turbulent heat conductivity, $\frac{dT}{dz}$: air temperature gradient at the air-ice interface)

We approximate the air temperature gradient at the air-ice interface with the finite difference:

$$\frac{dT}{dz} \approx \frac{T_a - T_{ai}}{\Delta z} \tag{3}$$

(T_a: air temperature at height Δz above the air ice interface, T_{ai}: air-ice interface temperature,)

The turbulent heat conductivity is unknown and depends on the magnitude of the turbulence. The magnitude of the turbulence depends on the wind speed. And the wind speed depends on the ventilation rate (u) in the tank. Here, we assume a linear relationship between all terms, such that $\kappa_t \propto u$. However, this assumption may need to be reformulated in future studies (see discussion). Combining all constants in the proportionality constant λ_a (hereafter referred to as turbulent conductivity), the turbulent heat flux is given by:

$$Q_a = -\lambda_a u (T_a - T_{ai}) \tag{4}$$

. The enthalpy flux from the water into the ice seems to be of less concern, since the tank is neither heated nor cooled from below. Hence, the enthalpy flux comes solely from cooling the water to the freezing point. As the water temperature is always close to the freezing point and the enthalpy of fusion is much larger than the enthalpy of cooling the water to the freezing point, we assume that the water heat flux is small. Nevertheless, we include the enthalpy that needs to be dissipated in order to cool the water to the freezing point in the latent heat of fusion:

$$L^* = L + \frac{\rho_w}{\rho_i} c_w \left(T_w - T_f\right) \tag{5}$$

(L^*: modified latent heat of fusion, ρ_w: density water, c_w: heat capacity water, T_w: water temperature, T_f: freezing point).

In order to calculate the turbulent heat flux (Eq. 2) we need to know the temperature at the air-ice interface. This temperature depends on the insulation of the ice. Physically, the insulation of the ice depends on its thermal conductivity (λ_i) and on its thickness. We assume that the thermal conductivity of both ice layers is similar. We compute the air-ice interface temperature (Eq. 5) by equating the turbulent heat flux (Eq. 2) with the enthalpy flux in the inside of the ice (Eq. 4).

$$Q_i = -\frac{T_{ai} - T_f}{h} \tag{6}$$

$$T_{ai} = \frac{\lambda_a u h T_a + \lambda_i T_f}{\lambda_a u h + \lambda_i} \tag{7}$$

(Q_i: heat flux in the ice, λ_i: thermal conductivity ice).

Finally, in order to obtain the ice growth model, we combine (Eq. 1), (Eq. 2), and (Eq. 5). The resulting differential equation (Eq. 6) has an analytical solution for a constant water temperature and a constant ventilation rate (Eq. 7). We denote that this ice growth model approach is similar to the historical approach of Anderson (1961), except of the slightly different turbulent heat flux and the modified latent heat of fusion.

$$\rho_i L^* \frac{dh}{dt} = \lambda_i \lambda_a u \frac{T_f - T_a}{\lambda_i + \lambda_a u h} \tag{8}$$

$$h(\theta) = \sqrt{\left(h_0 + \frac{\lambda_i}{\lambda_a u}\right)^2 + 2\frac{\lambda_i}{\rho_i L^*}\theta} - \frac{\lambda_i}{\lambda_a u} \tag{9}$$

$$\theta = \int_{t_0}^{t} T_f - T_a dt' \tag{10}$$

(θ: freezing degree days)

For modeling ice growth in the HSVA, we divide the ice growth into three stages. In the first stage the granular ice layer grows. In the second stage the columnar ice layer grows with a ventilation rate of 0.6. In the third stage the cooling is turned off and the columnar layer grows with a ventilation rate of 0.2.

Prediction of cooling duration

To predict the amount of ice growth, we also need to predict the air temperature development. Figure 2 shows a typical air temperature profile that was measured during an ice sheet production. The evolution of the temperature can be separated into five different phases. It starts with the pre-cooling, all ice that grows during this phase is removed at the end of this phase. Afterwards, the seeding is performed. Since the thermometer need to be lifted for the seeding, a jump in the temperature curve is visible during this phase. In the cooling phase a large part of the columnar ice grows. Once the ice thickness is close to the desired thickness, the temperature is raised to a tempering temperature (tempering phase). Finally, in the last phase, the experiments on the ice are performed. Ice growth takes place in phases 2 to 4. We assume, that the amount of ice that grows during the second phase is always the same. For this reason, the ice growth model starts in phase 3 with a constant initial ice thickness.

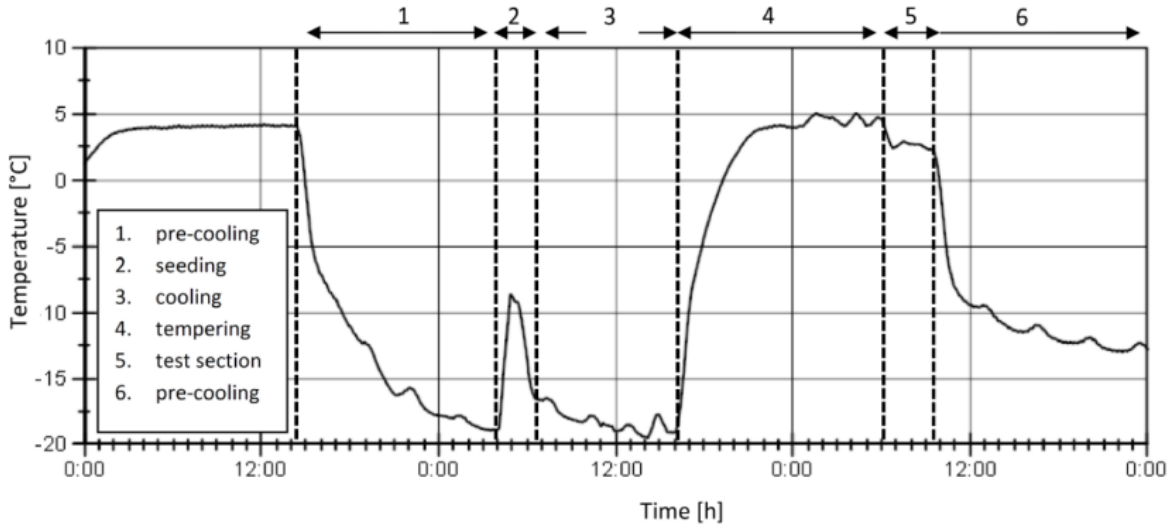

Figure 2. Phases of ice growth. The graph shows the air temperature as a function of time during a production of an ice sheet at HSVA.

The prediction model predicts the cooling duration t_c, that is the duration until the air cooling is turned off (temperature peak in phase 2 until the end of phase 3), as a function of the desired ice thickness. The initial air and water temperature must be provided to the prediction model. We assume that the air temperature stays constant during cooling and then exponentially approaches the tempering temperature after the cooling is turned off (Eq. 9).

$$T(t) = \begin{cases} T_c & \text{for } t < t_c \\ T_t + (T_c - T_t)e^{-\tau(t-t_c)} & \text{for } t \geq t_c \end{cases} \tag{11}$$

(T_c: cooling temperature, T_t: tempering temperature, t_c: cooling duration, τ: time constant)

In order to calculate the cooling duration, we first calculate the amount of ice that grows or melts during the tempering phase (the ice post growth). By subtracting the ice post growth from the desired ice thickness, we obtain the ice thickness at the end of the cooling phase ($h' = h - \Delta h$). Finally we invert the ice growth equation (Eq. 7) to get the cooling duration that is needed to grow ice of the thickness h'. The amount of ice that grows or melts during the tempering phase (ice post growth) depends on the final tempering temperature (T_t) and on the tempering duration t_t (Fig. 2: Duration of phase 4). For this reason, these two parameters need to be provided to the prediction model. By inserting (Eq. 9) in (Eq. 7) and (Eq. 8), we calculate the ice post growth from (Eq. 10).

$$\Delta h = h + \frac{\lambda_i}{\lambda_a u} - \sqrt{\left(h + \frac{\lambda_i}{\lambda_a u}\right)^2 - 2\frac{\lambda_i}{\rho_i L^*}\theta_t} \tag{12}$$

$$\theta_t = (T_f - T_t)t_t + \frac{T_c - T_t}{\tau}(e^{-\tau t_t} - 1) \tag{13}$$

(h: desired final ice thickness, Δh: ice post growth, θ_t: freezing degree days during temperature adjustment)

During cooling the freezing degree days are given by:

$$\theta_c = (T_f - T_c)(t_c - t_0) \tag{14}$$

(t_c: cooling duration, t_0: growth duration of granular ice layer).

Finally, by inverting (7) from $h'(\theta_c)$ to $\theta_c(h')$ and using (12), we obtain the predicted cooling duration:

$$t_c = t_0 + \frac{\rho_i L^*}{2\lambda_i} \frac{1}{T_f - T_c} \left(h'^2 - h_0^2 + 2 \frac{\lambda_i}{\lambda_a u} (h' - h_0) \right) \quad (15)$$

(h_0: thickness of granular layer).

Table 1. List of model parameters

Parameter		Value
Salinity (Water)	S_w	7 psu
Density (Water)	ρ_w	1005 kg m^{-3}
Heat Capacity (Water)	c_w	4.22 kJ kg^{-1} K^{-1}
Density (Ice)	ρ_i	890 kg m^{-3}
Thermal Conductivity (Ice)	λ_i	1.943 W m^{-1} K^{-1}
Freezing Point	T_f	-0.379 °C
Latent Heat of Fusion	L	306 kJ kg^{-1}
Initial Ice Thickness	h_0	3.34 mm
Starting Time	t_0	35 minutes
Time constant (Thick Ice / Thin Ice)	τ	$129.3 \cdot 10^{-6}$ s^{-1} / $428.7 \cdot 10^{-6}$ s^{-1}
Turbulent Conductivity	λ_a	19.47 W m^{-1} K^{-1}

Parameter estimation

For the ice growth prediction model, we need to determine model parameters. A list of all model parameters is given in table 1. While most model parameters can be directly measured, some parameters are hard to assess. In this section we focus on the determination of the initial ice thickness, of the starting time, of the turbulent conductivity coefficient, and of the time constant of temperature adjustment.

The starting time is the time at which the model starts to model the growth of the columnar ice layer. The starting time needs to be after the time at which the granular ice layer is fully grown. In our experience the granular ice layer grows within the first 30 minutes of ice growth. For this reason, we set the starting time to 35 minutes. To determine the initial ice thickness h_0, that is the ice thickness at the starting time, we measured the ice thickness after 35 minutes of ice growth.

In order to estimate the turbulent conductivity λ_a, we use existing measurements of air temperature, water temperature and ice thickness from previous ice sheet productions. For each ice sheet production, the ice thickness was measured when it reached its final thickness (after the temperature adjustment). For two ice sheet productions, the ice thickness was also measured multiple times during the growth. A total of 29 ice thickness measurements for 21 ice sheet

productions are available. Since no time stamps are available for the final ice thickness measurements, we estimated the time of measurement. To do this, we looked for temperature jumps in the temperature records. These jumps indicate that experiments have been carried out. We set the time of measurement shortly before these jumps. Measurements of air and water temperature are time series that start at the beginning of ice growth with a temporal resolution of one minute.

For the estimation of the turbulent conductivity, we define a residual function. The residual function returns the mean squared difference between measured and modeled ice thicknesses for a given turbulent conductivity (Fig 3b). We compute the modeled ice thickness from the measured air and mean water temperature (Eq. 7). To find the turbulent conductivity for which the residual function is minimal, we use the global optimization algorithm SHGO (Endres, et al., 2018). More detail on the implementation of the optimization algorithm can be found in (Rosenau, 2022).

With the parameters discussed so far, the ice thickness can be modeled for a given temperature time series. However, for the prediction model we need to predict the temperature curve. As discussed in the previous section, we assume that the temperature adjusts exponentially to the tempering temperature in phase 4 (Fig. 2). In order to find the time constant, we fit an exponential curve to the measured time series of the air temperature.

RESULTS AND DISCUSSION

In the first part of this section, we present the result of the estimation of the turbulent conductivity λ_a. In the second part of this section, we present results of a test application of this prediction model. We use the prediction model to predict the cooling time that is necessary to grow a 7 mm thick ice sheet.

Parameter estimation: Turbulent Conductivity

The minimal mean square difference between the measured and modeled ice thickness is 2.17 mm for a turbulent conductivity of 19.47 W m^{-1} K^{-1}. The deviation between measured and modeled ice thickness as a function of freezing degree days is shown in Figure 3. Thereby, the deviation seems to be normally distributed; There is neither a trend of overestimation nor of underestimation of ice thickness for different freezing times. Hence, the ice growth in the model agrees with the observed ice growth.

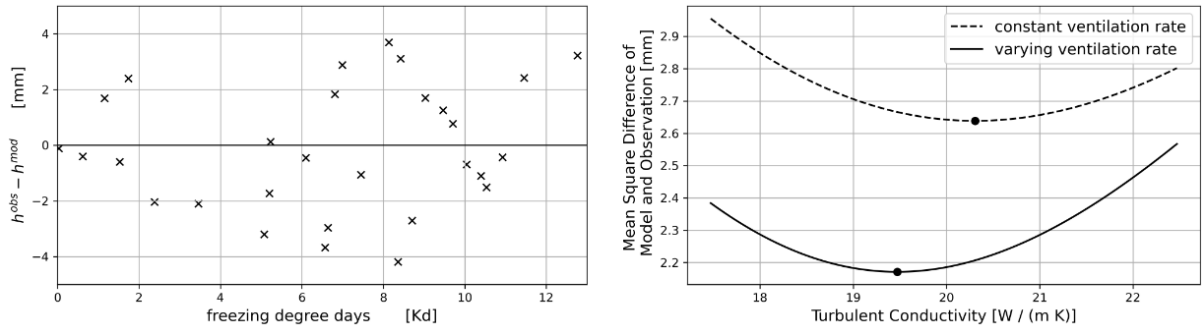

Figure 3. Results of the parameter estimation. Left: Difference between observed (h^{obs}) and modeled ice thickness (h^{mod}) for the best turbulent conductivity value (with varying ventilation rate). Right: Mean square difference between observed and modeled ice thickness as a function of the turbulent conductivity. The minima are marked with black dots.

The large mean deviation between modeled and observed ice thickness could either be due to

an oversimplified model, or due to inaccurate measurements. When the ice thickness is measured, the ice thickness is measured individually at several (about 100) different tank positions. The values that we use here for the observed ice thickness is the mean of these individual measurements. Although the measurement inaccuracies should be small since the number of individual measurements is large, we expect some inaccuracies since the ice thickness is measured by different persons at different days. And the measurement of the ice thickness still depends on the person that performs the measurement, i.e. how much the ice is compressed in the caliper reading. The accuracy may be estimate to be 1 mm.

However, we presume that most of the inaccuracy of the model is due to unknown measurement times. First, the starting time of ice growth that we use here could deviate from the actual value by approximately 15 minutes. For such low ice thicknesses as made in the HSVA, 15 minutes more or less of freezing time could mean half a millimeter more or less of ice thickness. Second, our estimation of the unknown timestamps of the final ice thickness might deviate from the actual time of measurements by multiple hours. Although the range of inaccuracy of the timestamp is within the tempering phase (when ice growth/melting is small), the resulting error on the modeled ice thickness can be a few millimeters.

Parameter estimation: Temperature adjustment phase

The temperature adjustment during the tempering phase differs between ice sheet productions of thin ice from the temperature adjustment during ice sheet productions of thick ice. With thin ice sheet productions, the temperature adjusts faster towards the tempering temperature than with thick ice sheet productions. The two different time constants are shown in table 1. We did not find the reason for those different adjustment speeds. However, we suspect that this is due to the cooling program that controls the air temperature. See (Rosenau, 2022) for a more detailed discussion on this.

Test of prediction model

In order to test the ice growth prediction model, we applied the model by predicting the cooling duration that is needed to grow ice that is 7mm thick. At the time of the experiment, less data was available for parameter estimation. For this reason, the parameters that we use for the prediction differ from those in table 1: We used a turbulent conductivity of 19.56 W m^{-1} K^{-1}, a starting time of 60 minutes, and an initial ice thickness of 3.56 mm. Further, we used a ventilation rate of $u = 0.6$ during cooling and during the temperature adjustment phase. For these parameters, the predicted cooling duration is 2 hours and 13 minutes.

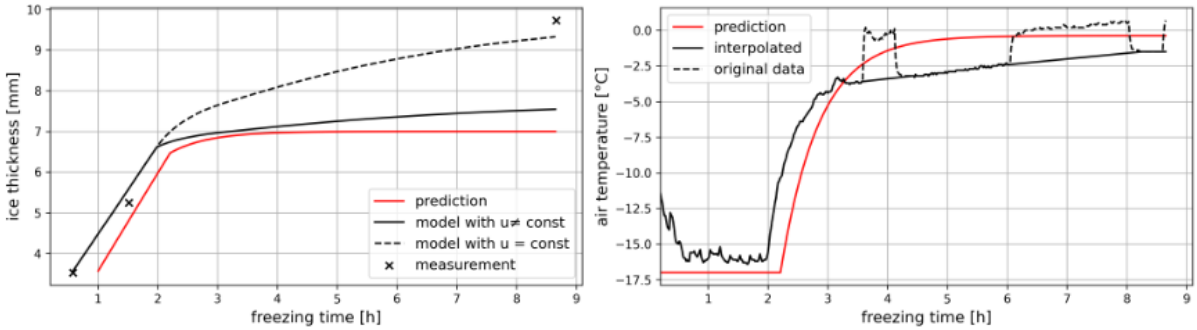

Figure 4. Predicted ice growth vs observed ice growth. Left: The red line is the predicted ice thickness, the black crosses are the observed ice thicknesses, and the black line is the modeled ice thickness from the measured air temperature. Right: The red line is the predicted air temperature; The black line is the measured air temperature. Note that the temperature is artificially large in 2 time intervals (dashed line) because we moved the thermometer for

other experiments. We use linear interpolation to fill the gaps.

Although the measured cooling temperature is about one degree warmer than our predicted cooling temperature, the final ice thickness is 2.7 mm thicker than the desired ice thickness. Thereby, the model underestimates the ice growth from the very beginning. The ice thickness of our first measurement after 35 minutes of ice growth is already as thick as the predicted ice thickness after 60 minutes of ice growth. For this reason, we stopped the cooling 13 minutes earlier than in our prediction.

For the experiment on the ice, it was important that the air temperature is always below the freezing point. For this reason, we stopped the inflow of warm air before the air temperature reached the freezing point. As a result, the air temperature was lower than in our prediction during temperature adjustment. This has led to a strong ice growth in the tempering phase. In order to test whether the model would have correctly predicted the ice growth with the measured temperature given, we modeled the ice thickness from the measured air temperature (Figure 4, solid black line). The modeled post-growth is stronger than in the prediction, but still much lower than the observed post growth.

We speculate that the underestimated ice growth during post growth can have two causes: First, the heat exchange between air and ice during the ice post growth phase is larger than expected, the turbulent ventilation rate may scale nonlinear with the ventilation rate and not linear as we assumed. Second, we neglected the thermal inertia of the ice. However, the ice may further grow when heat is transferred from the water to the ice in order to temper the ice. Further studies are necessary to quantify this impact.

Repeating the ice growth model with a constant ventilation rate results in a higher agreement between model and measurements (Figure 4, dashed black line). This result suggests that the heat exchange between air and ice is independent from the ventilation rate. However, repeating the parameter estimation with a constant ventilation rate yields worse results (Figure 3). The mean deviation between modeled and observed ice thickness increases. With a larger ventilation rate during temperature adjustment, the heat exchange between air and ice becomes stronger. Thus, the error in the measurement time of the ice thickness during this phase has a stronger impact on miscalculated ice thicknesses in the model.

To get a more accurate picture of the relationship between the ventilation rate and the heat exchange between air and ice, further measurements of the ice thickness during the temperature adjustment are necessary.

Transferability to other ice tanks

The presented model is developed for the model ice of HSVA which is columnar structured and grows into saline water with a salinity of 7ppt. Other ice tanks worldwide use either a different ice generation process to generate columnar or granular ice or a different dopant (e.g. salt, urea, ethanol) with different concentrations. An overview is found in von Bock und Polach et al. (2019). This growth model can only be transferred to ice tanks that use columnar model ice, where seeds let the ice grow into the water. However, as other tanks use different chemicals (dopants) to adjust the ice properties and different concentrations the presented model would need some readjustments. The size of the facilities might also play a role. Granular ice comes from layer-wise seeding of ice crystals, where ice undergoes very limited growth.

CONCLUSIONS

The mean squared difference between modeled and measured ice thickness is 2.17 mm. Since we tuned model parameters by minimizing the mean squared difference and thus a fit to measurement errors is likely, the value of 2.17 mm marks a lower boundary. However, we speculate that one major source of the deviation between model and measurement is due to uncertainties in the measurements. Nevertheless, the application of the prediction model showed that in particular the description of the ice growth during tempering has high discrepancies to the actual ice growth. Another reduction of prediction accuracy is expected to result from the simplified generic correlation between ventilation rate and heat flux.

One possibility to improve the modeling of ice growth during tempering is to separately describe the atmospheric heat flux in the cooling phase and in the tempering phase. However, this requires more accurate data. We suggest measuring the ice thickness three times for each ice cover in the future to improve estimation results. The first measurement should be taken shortly after the start of ice growth. It is important that this is always done at the same point in time relative to the start of cooling. This would allow testing the assumption of a constant initial ice thickness. If necessary, the model could be improved with a parameterization of the starting ice thickness. The other measurements should be made at the beginning and end of the tempering phase. This allows separate parameter estimations of the atmospheric heat flux during cooling and tempering.

REFERENCES

Anderson, D. L., 1961. Growth Rate of Sea Ice. *Journal of Glaciology,* Volume 3, p. 1170–1172.

Caldwell, D. R., 1978. The maximum density points of pure and saline water. *Deep Sea Research,* February, Volume 25, p. 175–181.

Endres, S. C., Sandrock, C. & Focke, W. W., 2018. A simplicial homology algorithm for Lipschitz optimisation. *Journal of Global Optimization,* March, Volume 72, p. 181–217.

Enkvist, E. & Makinen, S., 1984. A fine-grain model ice. *IAHR Ice Symposium, Hamburg,* p. 217–227.

Evers, K.-U., 1993. An Advanced TEchnique to Improve the Mechanical Properties of Model Ice Developed at the HSVA Ice Tank.. *Proc. of 12th POAC,* Volume 2, p. 877–888.

Haapala, J. & Lepparanta, M., 1996. Simulating the Baltic Sea ice season with a coupled ice-ocean model. *Tellus A,* October, Volume 48, p. 622–643.

Jasek, M., 2008. *Using new technology to understand water-ice interaction, Volume 2.* s.l., s.n.

Klein, M., Hartmann, M. & von Bock und Polach, F., 2021. Note on the Application of Transient Wave Packets for Wave–Ice Interaction Experiments. *Water,* June, Volume 13, p. 1699.

Lake, R. A. & Lewis, E. L., 1970. Salt rejection by sea ice during growth. *Journal of Geophysical Research,* January, Volume 75, p. 583–597.

Launiainen, J. & Cheng, B., 1998. Modelling of ice thermodynamics in natural water bodies. *Cold Regions Science and Technology,* June, Volume 27, p. 153–178.

Launiainen, J. & Vihma, T., 1990. Derivation of turbulent surface fluxes — An iterative flux-profile method allowing arbitrary observing heights. *Environmental Software,* September, Volume 5, p. 113–124.

Leppäranta, M., 1993. A review of analytical models of sea-ice growth. *Atmosphere-Ocean,* March, Volume 31, p. 123–138.

Maykut, G. A. & Untersteiner, N., 1971. Some results from a time-dependent thermodynamic model of sea ice. *Journal of Geophysical Research,* February, Volume 76, p. 1550–1575.

Millero, F. J., 1978. Freezing point of sea water. *eighth report of the Joint Panel of Oceanographic Tables and Standards, appendix,* Volume 6, pp. 29-31.

Monin, A. S., 1958. The Structure of Atmospheric Turbulence. *Theory of Probability {\&}amp$\mathsemicolon$ Its Applications,* January, Volume 3, p. 266–296.

Nkoko Nossa, A. & others, 2015. *Method for Prediction of Sea Ice Thickness Based on the Blowing Air Temperature and Speed,* s.l.: s.n.

Notz, D., 2003. Impact of underwater-ice evolution on Arctic summer sea ice. *Journal of Geophysical Research,* Volume 108.

Omstedt, A. & Wettlaufer, J. S., 1992. Ice growth and oceanic heat flux: Models and measurements. *Journal of Geophysical Research,* Volume 97, p. 9383.

Ono, N., 1967. Specific heat and heat of fusion of sea ice. *Physics of Snow and Ice: proceedings,* Volume 1, pp. 599-610.

Petrich, C. & Eicken, H., 2016. Overview of sea ice growth and properties. In: *Sea Ice.* s.l.:John Wiley & Sons, Ltd, p. 1–41.

Pringle, D. J., Eicken, H., Trodahl, H. J. & Backstrom, L. G. E., 2007. Thermal conductivity of landfast Antarctic and Arctic sea ice. *Journal of Geophysical Research,* April.Volume 112.

Rosenau, S. G., 2022. *Bachelor Thesis: Development of Model Ice Growth Prediction Model.* s.l.:Universität Hamburg.

Schwarz, J. & Weeks, W. F., 1977. Engineering Properties of Sea Ice. *Journal of Glaciology,* Volume 19, p. 499–531.

Stefan, J., 1890. Über die Theorie der Eisbildung insbesondere über Eisbilding im Polarmeere. *Ber. Kais. Akad. Wiss. Wein,* Volume 98, p. 965.

Virtanen, P. et al., 2020. SciPy 1.0: fundamental algorithms for scientific computing in Python. *Nature Methods,* February, Volume 17, p. 261–272.

von Bock und Polach, F., Klein, M. & Hartmann, M., 2021. A New Model Ice for Wave-Ice Interaction. *Water,* December, Volume 13, p. 3397.

von Bock und Polach, R. U. F. et al., 2019. The non-linear behavior of aqueous model ice in downward flexure. *Cold Regions Science and Technology,* September, Volume 165, p. 102775.